Direct-Write Assembly of 3D Hydrogel Scaffolds for Guided Cell Growth

By *Robert A. Barry III, Robert F. Shepherd, Jennifer N. Hanson, Ralph G. Nuzzo, Pierre Wiltzius,* and *Jennifer A. Lewis**

The ability to pattern soft materials at the microscale is critical for several emerging technologies, including tissue-engineering scaffolds,[1–3] photonic crystals,[4–6] sensors,[7–9] and self-healing materials.[10] Hydrogels are an important class of soft materials that can be fabricated in the form of 3D microperiodic structures by colloidal templating[3,7–9,11] or interference lithography.[12] However, neither approach allows one to omnidirectionally vary the spacing between patterned features over length scales ranging from sub-micrometer to tens of micrometers. By contrast, direct-write assembly enables a wide array of materials to be patterned in nearly arbitrary shapes and dimensions.[13–15] Here, we report the fabrication of 1D and 3D microperiodic hydrogel scaffolds by direct-write assembly of an acrylamide-based ink. For the first time, we combine direct ink writing with in situ photopolymerization to obtain hydrogel scaffolds with micrometer-sized features (see Fig. 1). By plating 3T3 murine fibroblasts onto one-, two-, and four-layer hydrogel scaffolds, we demonstrate their cytocompatibility and, hence, potential suitability for tissue-engineering applications.

Direct ink writing (DIW) is a layer-by-layer assembly technique in which materials are patterned in both planar and 3D forms with lateral feature sizes that are at least an order of magnitude smaller than those achieved by ink-jet printing[16–18] and other rapid prototyping approaches,[19–24] and nearly comparable in size to those produced by two-photon polymerization[25] and interference holography.[12] Central to our approach is the creation of concentrated inks that can be extruded through fine deposition nozzles in filamentary form, and then undergo rapid solidification to maintain their shape even as they span gaps in the underlying layer(s). Unlike prior efforts on polyelectrolyte inks that required reservoir-induced coagulation to enable 3D printing,[14] we report the creation of hydrogel inks that can be printed directly in air, where they undergo solidification via photopolymerization (see Fig. 1a and b).

The ink is created by first mixing monomeric acrylamide, glycerol, and water. Upon ageing for several hours under ambient conditions, the monomeric species polymerizes to yield a gel composed of 30 w/o polyacrylamide chains.[26] ^{1}H NMR reveals that peaks associated with acrylamide, which are initially present, disappear after polymerization, followed by the emergence of two new peaks that correspond to alkyl chains (data not shown). Concomitantly, as the solution ages, sharp rises in both the shear elastic, G', and loss, G'', moduli are observed, suggesting that the resulting gel is composed of physically entangled polyacrylamide chains (see Fig. 2a). To determine their degree of polymerization, N, the intrinsic viscosity, $[\eta]_0$, of diluted polymer solutions is measured by capillary viscometry, and found to be $[\eta]_0 \approx 270\,\mathrm{mL\,g^{-1}}$ (see Fig. 2b).[27,28] Using the Mark– Houwink relation, $[\eta]_0 = KM^a$, their molecular weight is determined to be $8.9 \times 10^5\,\mathrm{g\,mol^{-1}}$, where K is 9.3×10^{-3} and a is taken to be 0.75 for polyacrylamide dissolved in an aqueous solution (0.5 M NaCl)[29–31]. Hence, this initial polymerization process yields polyacrylamide chains with an average degree of polymerization $N = 1.3 \times 10^4$ that is well above the entanglement value of $N_e = 128$.[32]

To further optimize the ink for direct-write assembly, this polymerized mixture is diluted by adding monomeric acrylamide, a crosslinking agent, *N*, *N* methylene bisacrylamide, a photoinitiator, diethoxyacetophenone, and deionized water at weight ratios (w/w) of 0.480, 0.036, 0.004, and 0.480, respectively. Notably, the initial polymerization step could be eliminated simply by adding high-molecular-weight polyacrylamide chains

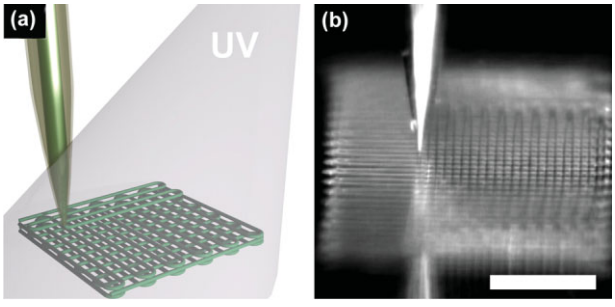

Figure 1. a) Schematic illustration of direct writing of a hydrogel-based ink through a gold-coated deposition micronozzle that is simultaneously photopolymerized via UV illumination. b) Optical image of a 3D hydrogel scaffold acquired during direct ink writing. Scale bar: 200 μm.

[*] Prof. J. A. Lewis, R. F. Shepherd
Department of Material Science and Engineering
University of Illinois
1304 W Green St., Urbana, IL 61801 (USA)
E-mail: jalewis@illinois.edu
R. A. Barry III, Prof. P. Wiltzius
Department of Material Science and Engineering
University of Illinois
1304 W Green St.
Urbana, IL 61801 (USA)
J. N. Hanson, Prof. R. G. Nuzzo
Department of Chemistry, University of Illinois
Department of Material Science and Engineering
University of Illinois
A128 Chemical & Life Sciences Laboratory
600 South Mathews Ave.
Urbana, IL 61801 (USA)

DOI: 10.1002/adma.200803702

© 2009 WILEY-VCH Verlag GmbH & Co. KGaA, Weinheim

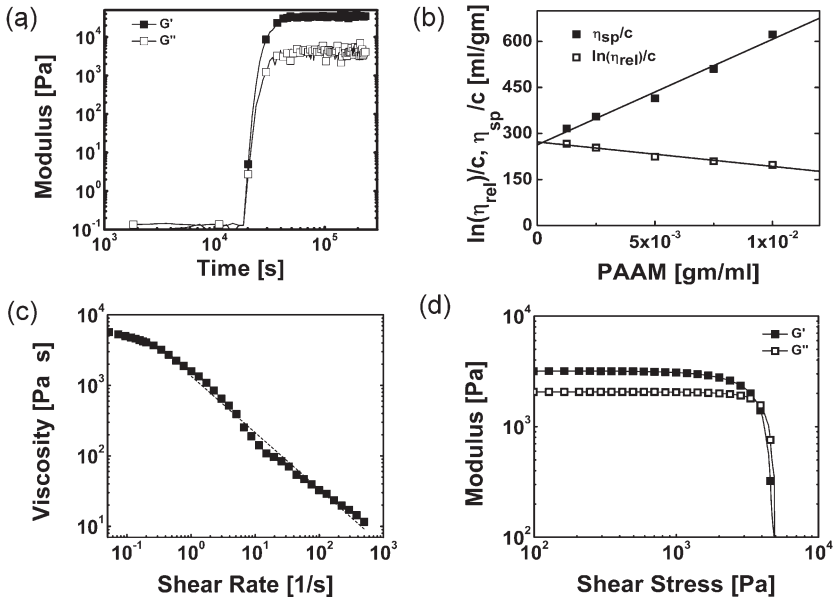

Figure 2. a) Shear elastic (G') and loss (G'') moduli as a function of polymerization time for the initial ink composed of acrylamide, glycerol, and water, b) specific and relative viscosity of the dilute polymer solutions of varying polyacrylamide concentration, c) apparent viscosity as a function of shear rate for final hydrogel-based ink, and d) shear elastic and loss moduli as a function of shear stress for the final hydrogel-based ink.

($\sim 10^6$ g mol^{-1}) directly to this photopolymerizable solution. The final ink formulation exhibits pronounced shear thinning behavior, which facilitates its flow through fine deposition nozzles (see Fig. 2c). For example, when the ink is printed through a 5 μm nozzle at 0.5 mm s^{-1}, which corresponds to an estimated shear rate of 100 s^{-1}, its viscosity is approximately 10 Pa · s. Under these conditions, the ink viscosity is nearly three orders of magnitude smaller than that observed at low shear rates ($\leq$0.1 s^{-1}). Upon diluting the ink, its shear elastic modulus decreases by about an order of magnitude, to $\sim 3 \times 10^3$ Pa, relative to its initial state (see Fig. 2d). Although this elasticity is sufficient for patterning 3D microperiodic scaffolds, the printed ink filaments must be further stiffened to prevent subsequent deformation, which occurs when the build times exceed several minutes. To obviate this, we have modified the direct writing process by mounting a fiber-optic guide onto the printhead, which facilitates in situ photopolymerization of the ink after it exits the gold-coated micronozzle (see Fig. 1a). The metallic coating prevents the ink from prematurely crosslinking within the glass nozzle due to UV illumination, thereby avoiding clogging during the printing process.

Using this modified DIW process, we pattern hydrogel scaffolds with precisely defined filament diameter, spacing, number of layers, and geometry. As a first example, we created hydrogel scaffolds composed of 5 μm filaments with a 20 μm spacing between filaments with 1–4 layers and a total area of 5 mm^2 (see Fig. 3a and b). To further demonstrate the capability of this novel approach, hydrogel scaffolds were printed with nominally 1 μm filaments with 5 μm spacing between filaments and six layers with a total area of 1 mm^2, as shown in Figure 3c. In this case, the hydrogel scaffolds are patterned in a face-centered tetragonal structure, in which the individual filaments are observed to span distances approximately five times their diameter with minimal deflection (see Fig. 3c, inset).

To determine their suitability for tissue-engineering applications, 3T3 murine fibroblast cells are plated onto a flat glass substrate (control) as well as 1D and 3D microperiodic hydrogel scaffolds. Poly-d-lysine is absorbed into the hydrogel scaffold network prior to cell seeding to enhance their cytocompatibility.[33] The fibroblasts plated on the control substrate display the typical flattened-out morphology shown in Figure 4a. By contrast, cell interactions with the underlying glass substrate and patterned features result in their alignment along the patterning direction of the 1D microperiodic hydrogel scaffolds, as shown in Figure 4b. This type of elongated morphology is similar to that observed by Zhang et al.,[34] in which murine fibroblasts formed aligned cell arrays on 1D periodic patterned surfaces that were biofunctionalized by microcontact printing of a self-assembling oligopeptide monolayer. We observed atypical fibroblast morphology in response to the 3D microperiodic hydrogel scaffolds (see Fig. 4c and d), in which fibroblast cells integrate themselves into the regions between interconnecting hydrogel filaments. Typically, one, or at most two, cells reside in this space between filaments, essentially compartmentalizing themselves. We find that the cells tend to sit in the square well created by interconnected filaments and then grow down into the scaffold towards the underlying glass substrate. Additionally, when the fibroblasts are in neighboring compartments, we observe interactions between the filaments of adjacent fibroblast cells (see Fig. 4d).

In summary, we have designed a new polymeric ink composed of physically entangled poly(acrylamide) chains in a photopolymerizable acrylamide solution that can be directly patterned in air

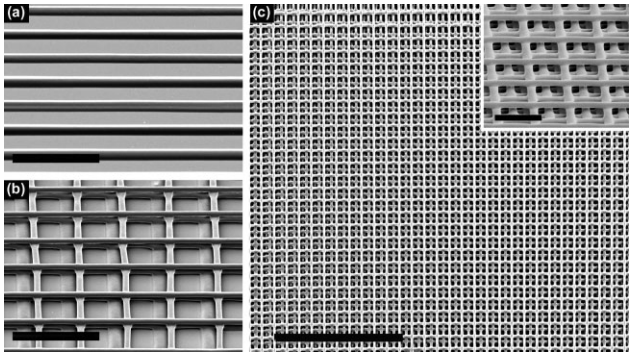

Figure 3. a) SEM image of 1D scaffold composed of 5 μm filaments with a 20 μm center-to-center spacing. b) 3D microperiodic hydrogel scaffold (four layers) composed of 5 μm filaments with a 20 μm center-to-center spacing. c) 3D microperiodic hydrogel scaffold (six layers) composed of nominally 1 μm filaments with a 5 μm center-to-center spacing. The inset in c) shows a higher-magnification tilted view of this scaffold. Scale bars are 50 μm (a–c), and 6 μm (inset), respectively.

WILEY InterScience DISCOVER SOMETHING GREAT
© 2009 WILEY-VCH Verlag GmbH & Co. KGaA, Weinheim

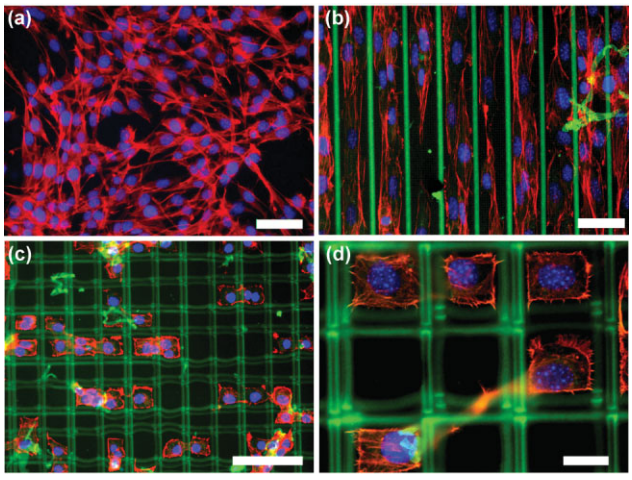

Figure 4. Optical fluorescence microscopy images of 3T3 fibroblasts plated on the a) flat glass control, b) 1D microperiodic hydrogel scaffold, and c,d) 3D microperiodic hydrogel scaffolds (four layers). d) Higher-magnification view of c) demonstrating the interaction between neighboring cells. In these images, rhodamine–phalloidin stains the actin red, DAPI stains the DNA nucleus blue, and the hydrogel scaffolds fluoresce green through the incorporation of fluorescein-o-acrylate. Scale bars are 100 μm (a–c) and 20 μm (d), respectively.

via a combination of direct-write assembly and in situ photocuring. This novel ink design can be readily extended to other chemistries, including those more suitable for tissue-engineering scaffolds, such as poly(2-hydroxyethyl methacrylate).[35] The ability to create hydrogel scaffolds with microscale features in both planar and 3D forms opens a new avenue for tailoring scaffolds for a broad array of applications, including tissue engineering, tunable optical sensors, and stimuli-responsive soft materials.

Experimental

Material System: The ink was initially formed by mixing 1 mL deionized water (Milli-Q, Millipore), 5 g of glycerol (Sigma Aldrich), and 3.5 g acrylamide (Acros). These constituents were magnetically stirred at 30 °C until the acrylamide was fully dissolved. In the quiescent state, this solution underwent spontaneous polymerization within hours to days. If the polymerization was slow, 0.1 M $MgCl_2$ was added as a catalyst. After this process was complete, 2 mL of deionized water were added to this highly viscous solution. A separate solution was produced by mixing 5 mL deionized water, 5 g acrylamide (Acros), 0.3 g methylene bisacrylamide (MP Biomedicals), 0.04 mL diethoxyacetophenone (Acros), and 0.018 g Fluorescein O-acrylate (Sigma Aldrich). 2 μL of this second solution was added in 0.5 mL aliquots to polymerized solution until the desired rheological properties were attained. The fluorescently labeled monomer was incorporated to facilitate direct imaging of the patterned scaffolds after the cell culture was complete.

NMR Analysis: ^{1}H NMR measurements were carried out using a Varian Unity 400. The sample was prepared identically to the initial ink formulation; however, D_2O was used instead of deionized water to generate an improved signal with better alignment. Specifically, 1 mL D_2O, 5 g of glycerol (Sigma Aldrich), and 3.5 g acrylamide (Acros) were mixed together in solution. These constituents were magnetically stirred at 30 °C until the acrylamide was dissolved. Samples were analyzed prior to and post polymerization with NUTS (Acorn NMR) software package.

Ink Rheology: Oscillatory rheometry was performed on the initial ink solution using a cup and bob geometry at a frequency of 1 Hz and shear stress of 1 Pa. Oscillatory rheometry was also performed on the final ink mixture at 1 Hz at a shear rate range from 0 to 200 s^{-1} to determine the elastic modulus (G'), loss modulus (G''), and yield stress (τ_y) of the printable ink. Viscometry was performed on the final ink mixture, from shear rates of 0 to 200 s^{-1}. All data were taken using a cup and bob geometry (C15; Bohlin) with 3 mL of material on a Bohlin CVOR controlled-stress rheometer.

Capillary rheology was performed by first dissolving the initial ink solution after polymerization was completed in water and then precipitating the polyacrylamide by immersion in ethanol [36]. The monomeric acrylamide and glycerol were soluble in ethanol, while poly(acrylamide) was not. This process was repeated several times, while concomitantly ultrasonicating the solution to facilitate dissolution. The precipitated polymer was then dissolved at varying concentrations in an aqueous solution containing 0.50 M NaCl [37]. The relative and specific viscosities of these diluted polymer solutions were then measured as a function of flow time using an Ubbelholde viscometer in a constant-temperature bath held at 26.5 ± 0.2 °C. The intrinsic viscosity was determined by measuring the flow values at different concentrations and using both the Huggins (Eq. 1) and Kraemer (Eq. 2) relationships: [31]

$$\frac{\eta - \eta_s}{\eta_s c} = [\eta] + k_H[\eta]^2 c \quad (1)$$

$$\frac{\ln(\eta/\eta_s)}{c} = [\eta] + \left(k_H - \frac{1}{2}\right)[\eta]^2 c \quad (2)$$

where η_s is the solvent viscosity, η the apparent viscosity, c the polymer concentration, and k_H is the Huggins coefficient. By extrapolating these equations to $c = 0$, the intrinsic viscosity was determined [38,39].

Direct-Write Asssembly of Hydrogel Scaffolds: Micropipette tips (World Precision Instruments) with diameters ranging from 1 to 10 μm were coated with a thin gold film (200 nm thick) to prevent photopolymerization of the ink prior to exiting the deposition nozzle. The micropipettes were mounted onto a rotating holder to ensure an even coverage, and coated inside a metal evaporator (Denton Vacuum DV-5024). Coverslip substrates were cleaned in piranha (sulfuric acid, hydrogen peroxide) solution for 1 h, rinsed with deionized water, and dried with nitrogen. Coverslips were placed in a 98% toluene (Fisher Scientific), 2% 3-(trimethoxysilyl)propyl methacrylate (Acros) solution for 18 h at 60 °C. The slides were removed just prior to drawing, rinsed with isopropanol, and dried. The ink was loaded into a syringe with an attached gold-coated tip in place. Once the substrate was leveled, ink flow was initiated by applying a pressure of 70–80 psi (1 psi = 6894.76 Pa). After the flow had begun, the pressure was reduced to 20–30 psi and the patterning was initiated. The printed scaffolds were defined by filament width, spacing between filaments, total patterned area, number of layers, and their geometry. We created both planar and 3D scaffolds with 1 to 5 μm filaments and a 5 to 20 μm spacing between filaments over 5 mm^2 areas with 1–6 layers. A UV lamp (Omnicure S200; Exfo) with a λ = 320–400 nm was used to expose the patterned structure to 5 mW cm^2 during the deposition process. Once patterning was complete, the scaffolds were exposed to a higher-intensity UV light source, ~400 mW cm^{-2}, for 20 min to ensure a fully photocured structure. To drive off excess water and enhance scaffold rigidity, each scaffold was then heated to 100 °C for 18 h.

Scaffold Imaging: The printed hydrogel scaffolds were soaked in deionized water for three days prior to cell culture to leach out glycerol and any unpolymerized acrylamide. Reflected-light optical microscopy (IX71; Olympus) was performed prior to cell plating to ensure structural integrity of the scaffolds. SEM images were obtained using a Philips XL30 ESEM-FEG; structures were dried and sputter-coated with gold prior to imaging.

3T3 Fibroblast Seeding and Imaging: The interaction of murine NIH/3T3 fibroblast cells with the printed hydrogel scaffolds was investigated to

© 2009 WILEY-VCH Verlag GmbH & Co. KGaA, Weinheim

assess their cytocompatibility. The initial cell stock (density of $\sim 1 \times 10^6$ cells mL^{-1}) was divided between three T-75 cell culture flasks, to which 20 mL of cell media (Dulbecco's Modified Eagle Medium, DMEM) that consisted of 4.5 g L^{-1} glucose, 4 mM glucose, 1 mM sodium pyruvate, 1.5 g L^{-1} sodium bicarbonate, and supplemented with 10% fetal bovine serum (FBS, Colorado Serum Company) and 100 U mL^{-1} penicillin/100 μg mL^{-1} streptomycin (Sigma Aldrich) was added. The media was exchanged the next day to remove excess dimethyl sulfoxide (DMSO, Sigma Aldrich). Cells were grown in a humidified incubator at 37 °C with 5% CO_2.

Hydrogel scaffolds were sterilized prior to cell plating through UV-light exposure in the laminar flow hood for 20 min. Scaffolds were immersed in 100 μg mL^{-1} poly-d-lysine (Sigma Aldrich) for 60 min prior to seeding. Flat glass coverslips were also evaluated as controls. Cells were plated onto the scaffolds at approximately 0.5×10^6 cells mL^{-1}, and allowed to proliferate for approximately 48 h. After two days in culture, the fibroblasts were rinsed three times with PBS, immersed in 4% paraformaldehyde at room temperature for 10 min, and then rinsed again with PBS. A PBS solution containing 0.25% Triton X-100 was placed on the cells for 3 min to permeate their membranes, and the samples were then rinsed again with PBS. The cells were incubated in 1% bovine serum albumin (BSA, Sigma Aldrich) in PBS for 10 min. The cells were then incubated for an additional 20 min in a rhodamine–phalloidin (Invitrogen Molecular Probes) solution diluted 1:200 in 1% BSA solution, and again rinsed with PBS. Finally, the samples were incubated with 0.002% DAPI in PBS (4′,6-diamidino-2-phenylindole, Invitrogen Molecular Probes) for 1 min and rinsed with deionized water. The rhodamine–phalloidin stains actin filaments red, while the DAPI stains the DNA in the nucleus blue. All fluorescent microscopy was performed using the Zeiss Axiovert 200 M inverted microscope. A Dapi/Hoechts/AMCA filter (Chroma Technology) was used for the DAPI imaging, a Special Yellow Rhodamine/Cy3/Texas Red filter (Chroma Technology) was used for the rhodamine imaging, and the Piston GFP filter was used for imaging the autofluorescence in the hydrogel scaffold.

Acknowledgements

R. A. B. and R. F. S contributed equally to the ink development and scaffold fabrication, and J. N. H. carried out all cell work. This material is based on work supported by the NSF Center for Nanoscale Chemical-Electrical-Mechanical Manufacturing Systems (DMI-0328162), NSF (CHE-07-4153; JNH, RGN), and the U.S. Army Research Office (DAAD19-03-1-0227). The authors gratefully acknowledge use of the Center for Microanalysis of Materials (CMM) in the Frederick Seitz Materials Research Laboratory and the Imaging Technology Group at the Beckman Institute.

Received: December 15, 2008
Revised: January 10, 2009
Published online: March 26, 2009

[1] L. G. Griffith, G. Naughton, *Science* **2002**, *295*, 1009.
[2] S. Ghosh, S. T. Parker, X. Wang, D. L. Kaplan, J. A. Lewis, *Adv. Funct. Mater.* **2008**, *18*, 1.
[3] J. Lee, M. J. Cuddihy, N. A. Kotov, *Tissue Engineering Part B* **2008**, *14*, 61.
[4] M. Campbell, D. N. Sharp, M. T. Harrison, R. G. Denning, A. J. Turberfield, *Nature* **2000**, *404*, 53.
[5] M. Deubel, G. V. Freynmann, M. Wegener, S. Pereira, K. Busch, C. M. Soukoulis, *Nat. Mater.* **2004**, *3*, 444.
[6] G. M. Gratson, F. Garcia-Santamaria, V. Lousse, M. Xu, S. Fan, J. A. Lewis, P. V. Braun, *Adv. Mater.* **2006**, *18*, 461.
[7] J. Holtz, S. Asher, *Nature* **1997**, *389*, 829.
[8] Y. J. Lee, P. V. Braun, *Adv. Mater.* **2003**, *15*, 563.
[9] R. A. Barry, P. Wiltzius, *Langmuir* **2006**, *22*, 1369.
[10] K. S. Toohey, N. R. Sottos, J. A. Lewis, J. S. Moore, S. R. White, *Nat. Mater.* **2007**, *6*, 581.
[11] Y. Liu, S. Wang, J. W. Lee, N. A. Kotov, *Chem. Mater.* **2005**, *17*, 4918.
[12] J. H. Kang, J. H. Moon, S. K. Lee, S. G. Park, S. G. Jang, S. Yang, *Adv. Mater.* **2008**, *20*, 3061.
[13] J. E. Smay, G. M. Gratson, R. F. Shepherd, J. Cesarano, III, J. A. Lewis, *Adv. Mater.* **2002**, *14*, 1279.
[14] G. M. Gratson, M. Xu, J. A. Lewis, *Nature* **2004**, *428*, 386.
[15] E. B. Duoss, M. Twardowski, J. A. Lewis, *Adv. Mater.* **2007**, *19*, 3485.
[16] P. Calvert, *Chem. Mater.* **2001**, *13*, 3299.
[17] T. H. J. van Osch, J. Perelaer, A. W. M. de Laat, U. S. Schubert, *Adv. Mater.* **2008**, *20*, 343.
[18] W. D. Teng, M. J. Edirisingh, J. R. G. Evans, *J. Am. Ceram. Soc.* **1997**, *80*, 486.
[19] E. Sachs, M. Cima, P. Williams, D. Brancazio, J. Cornie, *J. Eng. Ind. -Trans. ASME* **1992**, *114*, 481.
[20] J. Moon, J. E. Grau, V. Knezevic, M. J. Cima, E. M. Sachs, *J. Am. Ceram. Soc.* **2002**, *85*, 755.
[21] S. J. Hollister, *Nat. Mater.* **2005**, *4*, 518.
[22] G. Mapili, Y. Lu, S. Chen, K. Roy, *J. Biomed. Mater. Res. Part B Appl. Biomater.* **2005**, *75B*, 414.
[23] J. W. Lee, P. X. Lan, B. Kim, G. Lim, D.-W. Cho, *J. Biomed. Mater. Res. Part B: Appl. Biomater. Part B* **2008**, *87B*, 1.
[24] G. Vozzi, C. Flaim, A. Ahluwalia, S. Bhatia, *Biomaterials* **2003**, *24*, 2533.
[25] P. Tayalia, C. R. Mendonca, T. Baldacchini, D. J. Mooney, E. Mazur, *Adv. Mater.* **2008**, *20*, 1.
[26] A. I. Bol'shakov, D. P. Kiryukhin, *Polym. Sci. A* **2007**, *49*, 975.
[27] E. Pelletier, C. Viebke, J. Meadows, P. A. Williams, *Langmuir* **2003**, *19*, 559.
[28] R. A. Shanks, S. Wu, *J. Appl. Polym. Sci.* **2002**, *89*, 3122.
[29] J. Klein, K. D. Conrad, *Makromol. Chem.* **1980**, *181*, 227.
[30] T. Schwartz, J. Francois, G. Weill, *Polymer* **1980**, *21*, 247.
[31] M. Rubinstein, R. H. Colby, *Polymer Physics*, Oxford University Press, New York **2003**.
[32] R. S. Porter, *Makromol. Chem. Theory Simul.* **1992**, *1*, 119.
[33] R. J. Pelham, Y.-L. Wang, *PNAS* **1997**, *94*, 13661.
[34] S. Zhang, L. Yan, M. Altman, M. Lässle, H. Nugent, F. Frankele, D. A. Lauffenburger, G. M. Whitesides, A. Rich, *Biomaterials* **1999**, *20*, 1213.
[35] O. Wichterle, D. Li'm, *Nature* **1960**, *185*, 117.
[36] S. Wu, R. A. Shanks, *J. Appl. Polym. Sci.* **2004**, *93*, 1493.
[37] K. Lewandowska, *J. Appl. Polym. Sci.* **2007**, *103*, 2235.
[38] P. S. Russo, S. Siripanyo, M. J. Saunders, F. E. Karasz, *Macromolecules* **1986**, *19*, 2856.
[39] Y. Heo, R. G. Larson, *J. Rheology* **2005**, *49*, 1117.

WILEY InterScience® DISCOVER SOMETHING GREAT
© 2009 WILEY-VCH Verlag GmbH & Co. KGaA, Weinheim